NONLINEAR INTERACTIONS OF MULTIPLE LINEARLY UNSTABLE THERMOACOUSTIC MODES

Jonas P. Moeck* and Christian Oliver Paschereit

Institut für Strömungsmechanik und Technische Akustik
Technische Universität Berlin
Müller-Breslau-Strasse 8, 10623 Berlin, Germany
* Corresponding author: jonas.moeck@pi.tu-berlin.de

We investigate the dynamics of thermoacoustic systems with multiple unstable modes. If a linear analysis reveals more than one mode with positive growth rate, nonlinear methods have to be used to determine the existence and stability of steady-state oscillations. One possible way to engage this problem is a harmonic balance approach based on describing function representations for the flame response. In contrast to the case of a single unstable mode, the nonlinearity output to multiple sinusoidal components with different frequencies and amplitudes has to be known. Based on the harmonic balance approach, we present conditions for the existence and stability of single or multi-mode steady-state oscillations. We apply this method to a thermoacoustic model system having two linearly unstable modes. By varying one of the system parameters, we find stable and unstable single mode steady-states as well as unstable simultaneous oscillations. Associated with the stability of the single mode equilibrium solutions, we identify hysteresis in the oscillation type.

1 Introduction

Thermoacoustic instabilities remain a plaguing problem for gas turbine manufacturers. To assess the susceptibility to acoustically coupled instabilities, computational tools based on linearized models, incorporating experimentally or numerically determined flame response functions, are frequently used [14]. This type of analysis yields a set of unstable or marginally stable modes, which may be expected to exhibit oscillations. If more than one mode is found unstable, linearized theory can give no information on the dynamical characteristics that will be observed in the system. Typically it is assumed that one mode dominates the system dynamics so that there is one distinct oscillation with the other linearly unstable modes being suppressed. It somewhat suggests itself that the dominant mode will be the one with the largest linear growth rate. On the other hand, there is no sound argument to assume in general that the finite amplitude dynamics can be deduced from the properties of the linearized system.

One weakness of all linear models is their inability to give a reasonable estimate on the final oscillation amplitude. Also, the linear approach does not detect subcritical instabilities, for which the non-oscillating state is stable with respect to small perturbations, but a second stable equilibrium solution with finite amplitude exists [23]. Following a harmonic balance framework, describing function analysis [8], incorporating an amplitude dependent flame response into a linear acoustic model, has been used to calculate limit cycle oscillations in thermoacoustic systems [6] even bearing quantitative comparison with experimental data [10, 15]. The amplitude dependent flame response that is used in this type of analysis is a sinusoidal-input describing function, i.e., it represents the frequency and amplitude dependent gain and phase of a single input sinusoid while neglecting all harmonics. Discarding the higher frequency output of the nonlinearity does not introduce major errors because the system

acoustics typically have distinct bandpass character (associated with the mode frequencies), and the limit cycles will be found within the passbands.

Multiple unstable modes are not uncommon in thermoacoustic systems. A few relevant references will be mentioned in the following. In a model study of an annular combustion chamber, Schuermans et al. [19] found first and second order azimuthal modes to be linearly unstable. The time domain simulations showed only one mode oscillating in a limit cycle, though. When suppressing this mode by active control, the second unstable mode started to grow and settled on a finite amplitude oscillation.

In a recent paper, Stow and Dowling [21] investigated a similar configuration with a time domain network model. For certain geometrical parameters, a longitudinal (half-wave) and a first order azimuthal mode were found to be unstable. Running simulations with different initial conditions, they found the long time solution to settle on either of the two modes with the other being suppressed. In the transient regime, a significant growth of the eventually decaying mode could be observed. However, no stable state corresponding to simultaneous oscillations of the two linearly unstable modes was found in various simulation runs.

Identifying multiple linearly unstable modes in test-rig experiments is difficult. Observing only one oscillation mode does not necessarily mean that it is the only one unstable. As the references above indicate, there is clearly a tendency of one mode suppressing the other. In fact, this is an inherent property of two coupled oscillators with non-harmonically related frequencies, as will become clear later in the paper. Multiple peaks at non-harmonically related frequencies in pressure spectra were, e.g., explicitely mentioned by Gutmark et al. [9], Dunstan et al. [7], and Riley et al. [16] in test-rig studies and can be often found in measured engine spectra. It appears, however, difficult to judge whether these are indeed manifestations of simultaneously oscillating modes. Some of the peaks may be only noise driven resonances, and there is also the possibility that the system state is not stationary (in a non-statistical sense) but shares time between different attractors (limit cycles). The latter case will clearly exhibit more than one sharp peak in measured spectra, although no simultaneous oscillations exist.

It is also worth noting that experimental data often shows a markedly distinct transition from one oscillation mode to another when some control parameter is varied (see, e.g., Refs. [3, 13, 15]), and even hysteresis in the mode switching process may be involved. Then, most certainly, there is some transition region in which both modes are unstable (although only one is observed).

If we approach the problem of multiple linearly unstable thermoacoustic modes by considering it as equivalent to that of coupled oscillators, then there is a vast amount of literature available. One of the first to address this problem was van der Pol [22], in fact highlighting already some of the fundamental properties inherent to this type of system. In his study of a circuit with two oscillators and a nonlinear element, he noted that "the presence of one oscillation makes it more difficult for the other to develop". This he inferred by looking at what essentially can be identified as the dual-input describing function of a cubic term. Van der Pol used averaging arguments to identify four possible equilibrium solutions in the case of a cubic nonlinearity. In addition to the trivial solution, he found two equilibrium states at finite amplitude of only either of the oscillators and one combined mode corresponding to simultaneous oscillations. While the individual oscillation modes could be stable or unstable depending on the control parameter (the resonance frequency of one of the oscillators), the combined mode, if it existed, was always unstable. The hysteresis in the oscillation mode, which drew van der Pol's interest to this work initially, could be explained based on the stability of the individual oscillations.

The interaction of multiple unstable modes is a phenomenon that is relevant in various scientific branches (see,e.g., Refs. [2, 11]), but by far the most references are related to circuit theory. In this field, it was early recognized that for the determination of the stability of a particular limit cycle, perturbations by different modes have to be considered [1, 4]. For this and to determine possible simultaneous oscillation states [17], the single-input describing function is generally not sufficient. In the main part of the paper, we illustrate on the basis of an elementary configuration that this holds also true for thermoacoustic systems.

Multi-mode oscillations can be divided into two main classes: resonant (synchronous) and non-resonant (asynchronous), depending on the fact if phase interaction is important (or not). The latter case is present if the ratio of the mode frequencies is not a rational number (or if the common divisor is so large that phase coherence cannot be sustained in the presence of external and parametric noise). While the acoustic modes of idealized configurations may have eigenfrequencies which are multiples

of some fundamental mode, non-uniform cross-sectional areas and temperature distributions will typically render the case of harmonically related mode frequencies improbable for any real configuration. Therefore we consider only the asynchronous case in the following.

The rest of the paper is organized as follows. We introduce a harmonic balance approach for thermoacoustic systems with multiple unstable modes and derive conditions for steady-state oscillations and their stability. This method is applied to an elementary thermoacoustic model configuration with two linearly unstable modes. Based on this system, we illustrate the approach and show possible solution characteristics.

2 A harmonic balance approach for thermoacoustic systems with multiple unstable modes

We consider thermoacoustic systems with low Mach number mean flow, in which the heat release is coupled to the acoustic field in a quasi-one-dimensional way. In this case, perturbations in the heat release are solely induced by fluctuations in the axial particle velocity, and the expansion induced, in turn, only affects the axial flow divergence. Moreover, we can lump the complete acoustic field up- and downstream of the flame in equivalent admittance and impedance, $A(\omega)$ and $Z(\omega)$, which relate pressure and particle velocity on both sides of the flame. For such a system, the dispersion relation for linear fluctuations can be written as [18]

$$A(\omega)Z(\omega)\big(1+F(\omega)\big)-1=0, \tag{1}$$

where F is the transfer function from the upstream particle velocity to velocity divergence across the heat source. For compact flames, $F(\omega)$ is obtained from the heat release transfer function (relating fluctuations in heat release to those in approach flow) by invoking the low Mach number jump conditions [12]. Equation (1) has several solution branches ω_j, each of which is associated with an acoustic mode of the particular configuration. The imaginary part of ω_j determines if this mode is unstable and grows exponentially in time, or if it is damped. In the linear regime, the stability of one mode is independent of the presence of any other mode, clearly by eqn (1).

The linear dispersion relation is, however, only valid as long as the fractional velocity amplitude at the flame, $u_q = u/\bar{u}$, is small. At finite amplitude, the heat release response typically tends to saturate, and the gain decreases. This effect can be taken into account by means of a describing function [6,15], which endows the heat release transfer function with an additional dependence on the oscillation amplitude. In this case, the dispersion relation reads

$$A(\omega)Z(\omega)\big(1+F(\omega,a)\big)-1=0, \tag{2}$$

where a is the amplitude of the velocity oscillation at the flame. Solutions (ω_j, a_j) of (2) with $\mathrm{Im}\,\omega_j = 0$ correspond to steady state oscillations. In the presence of only one mode, the stability of this limit cycle can be inferred from the variation of the growth rate $-\mathrm{Im}\,\omega_j$ with amplitude. (We consider a Fourier transform such that $\partial_t \mapsto \mathrm{i}\omega$, with i denoting complex unity.) We assume here that the heat release response is the dominant source of nonlinearity and that the acoustic field can be considered as linear, even for finite amplitude oscillations. In gas turbine applications, in which the fractional pressure amplitudes typically do not exceed a few percent, this is commonly considered to be a sufficiently accurate approximation [6]. Acoustic boundary conditions are known to exhibit amplitude dependence at large particle velocities; this can be incorporated in this type of analysis, in principle [20].

2.1 Equilibrium solutions for multiple unstable modes

If more than one mode is oscillating with finite amplitude, the nonlinearity input, i.e., the normalized velocity fluctuation at the flame, u_q, is composed of several approximately sinusoidal signals with different frequencies, viz. $u_q = \sum_{n=1}^{M} a_n \sin\big(\mathrm{Re}(\omega_n)\,t+\theta_n\big)$. Since the nonlinearity acts on u_q rather than on the individual modes, clearly, the fundamental gain of one of the sinusoids will depend on the ampli-

tudes of all the others in general. Now assuming that the associated nonlinearity output (heat release or flow divergence) can be expanded in a multi-dimensional Fourier series with the $\mathrm{Re}\,\omega_n$ as basis frequencies, we can identify the gain of each input sinusoid as the corresponding Fourier coefficient of the output signal divided by the respective input amplitude. In this way, we obtain M multi-input describing functions $N_{a_n}(\boldsymbol{\omega},\boldsymbol{a})$, each of which depends on all other frequencies and amplitudes (which we have collected in vectors $\boldsymbol{\omega}$ and $\boldsymbol{a}$). The describing functions do not depend on the phases θ_n because we assumed only asynchronous oscillations. In this case, the phases of two sinusoidal signals (with non-rational frequency ratio) are essentially random variables [8] and therefore cannot have any influence on the fundamental harmonic gains. Although describing functions can be defined with respect to different types of signals, we consider only sinusoidal inputs in the present work.

For a static nonlinearity, it is always possible to expand the output signal in a multi-dimensional Fourier series. In case of a dynamic nonlinear relation, which is certainly the case for a flame, this is truly an assumption, excluding any subharmonic response, for instance, or intrinsic instabilities. This assumption is essentially identical to that necessary to represent a dynamic nonlinearity by a single-input describing function. The filtering hypothesis [1, 8] in the presence of multiple modes is stricter than for the single mode case. Low-pass character of the linear system is no longer sufficient because nonlinear combinations of the input signals also generate components at lower frequencies.

Adapting Choudhury and Atherton's results [4] to our case, we then have for multiple (M, say) modes at possibly finite amplitude the following set of dispersion relations

$$A(\omega_j)Z(\omega_j)\big(1+F_{a_j}(\boldsymbol{\omega},\boldsymbol{a})\big)-1=0,\quad j=1\ldots M. \tag{3}$$

We can consider this as an implicit relation, mapping the M amplitudes $\boldsymbol{a}$ to the complex frequencies $\boldsymbol{\omega}$. Steady-state oscillations are then characterized by purely real eigenfrequencies with corresponding non-zero amplitude. This covers the case of single-mode as well as simultaneous oscillations. The multi-input describing function F_{a_j} reduces to the single-input describing function if all amplitudes except for a_j are zero. Accordingly, single-mode equilibrium states can be computed with only the single-input describing function available (but stability cannot be assessed, as we will see below). For simultaneous steady-state oscillations, this is not so because more than one mode has finite amplitude, and the mutual interaction has to be taken into account when calculating the fundamental harmonic gains of the input sinusoids.

2.2 Stability of equilibrium solutions and transient dynamics

The conditions given above only determine possible (not necessarily stable) equilibrium states. To assess whether a certain steady-state oscillation is indeed realizable (observable in an experiment, say), stability with respect to perturbations in *all* relevant mode amplitudes must be considered. In the following, we will derive stability criteria applicable for the general case of multi-mode oscillations; single-mode oscillations are included as a special case.

Consider an equilibrium state $\boldsymbol{a}_{\mathrm{eq}}$ with $\tilde{M}$ non-zero elements. We call modes corresponding to non-zero amplitudes "participating" and denote these by $\tilde{\boldsymbol{a}}_{\mathrm{eq}}$ and the corresponding eigenfrequencies by $\tilde{\boldsymbol{\omega}}_{\mathrm{eq}}$. For the equilibrium state $\boldsymbol{a}_{\mathrm{eq}}$ to be stable, we certainly need $\mathrm{Im}\,\tilde{\boldsymbol{\omega}}^c_{\mathrm{eq}}>0$, where $\tilde{\boldsymbol{\omega}}^c_{\mathrm{eq}}$ is the complement of $\tilde{\boldsymbol{\omega}}_{\mathrm{eq}}$ relative to $\boldsymbol{\omega}$. In other words, the modes not participating in the oscillation $\boldsymbol{a}_{\mathrm{eq}}$ need to have a negative growth rate. In addition, $\boldsymbol{a}_{\mathrm{eq}}$ must be stable with respect to perturbations in the participating modes. Since these have zero imaginary part at $\boldsymbol{a}_{\mathrm{eq}}$, we need to assess the variation of the growth rates, $-\mathrm{Im}(\delta\tilde{\boldsymbol{\omega}})$, under a perturbation $\delta\tilde{\boldsymbol{a}}$. The stability of these perturbations is determined by the eigenvalues of $\mathbf{J}=\mathrm{Im}(\partial_{\tilde{\boldsymbol{a}}}\tilde{\boldsymbol{\omega}})$. Denoting the left hand sides of (3) for all participating modes by $\tilde{\boldsymbol{f}}$, we have by implicit differentiation

$$\mathbf{J}=-\mathrm{Im}\big[(\partial_{\tilde{\boldsymbol{\omega}}}\tilde{\boldsymbol{f}})^{-1}\partial_{\tilde{\boldsymbol{a}}}\tilde{\boldsymbol{f}}\big], \tag{4}$$

which can be computed explicitly. Then an equilibrium solution $\boldsymbol{a}_{\mathrm{eq}}$ is stable if $\mathrm{Im}\,\tilde{\boldsymbol{\omega}}^c_{\mathrm{eq}}>0$ and the eigenvalues of $\mathbf{J}$ have all positive real parts. (If at least one of the non-participating modes has zero growth rate or one eigenvalue of $\mathbf{J}$ has zero real part, $\boldsymbol{a}_{\mathrm{eq}}$ is a non-hyperbolic equilibrium, possibly at bifurcation, and stability has to be determined by higher order methods, which will not be considered

here.) The case of a single unstable mode is included; stability of a steady state oscillation then simply requires $\mathrm{Im}(\partial_a \omega) > 0$.

It is important to note here that, in case of multiple unstable modes, stability of a particular oscillation cannot be assessed based on knowledge of the single-input describing function only. This holds true even in the case of a single-mode oscillation. The reason is the following. Although the multi-input describing function F_{a_j} reduces to the single-input describing function if a_j is the only non-zero amplitude, computing the growth rate of another mode (k, say) requires to evaluate F_{a_k} for finite a_j. With the appropriate multi-input describing function available, however, the computation of the growth rates of all other modes with zero amplitude, as well as computing the eigenvalues of (4) is a straightforward task.

So far we only considered equilibrium states and their stability. If we, however, assume in addition that the oscillations vary slowly in amplitude (essentially an averaging condition which requires the interaction with the heat release to be small), then (3) will be representative also for the transient dynamics. For then the temporal evolution of the mode amplitudes can be obtained from

$$\dot{a}_j = -\mathrm{Im}\big(\omega_j(\boldsymbol{a})\big) a_j, \quad j = 1 \dots M, \tag{5}$$

where the ω_j depend on the oscillation amplitudes through the conditions (3). This will be particularly useful when considering the interaction of only two, maybe three unstable modes because the dynamics can be studied by means of a phase-plane analysis. If more than one stable oscillation exists, e.g., (5) can be used to estimate the individual basins of attraction.

Remarks

We should mention at this point that the type of analysis outlined in this section will be rather intricate to perform in any practical case if $M > 2$. This is mainly attributed to the multi-input describing function, that has to be available. Since F_a depends on all relevant frequency and amplitude combinations, numerical or experimental determination is virtually impossible. Even in the case of two modes, in which a dual-input describing function is necessary, the fundamental gain of each amplitude depends already on four parameters (ω_1, ω_2, a_1, and a_2).

3 Application to a model system

In this section, we study the dynamics of a model system with two linearly unstable modes. We do this for two reasons: (i) to demonstrate the harmonic balance approach outlined in the previous section and (ii) to illustrate some of the characteristic dynamics, which we conjecture to be rather general for thermoacoustic systems with multiple linearly unstable modes.

3.1 Model system definition

We consider the dynamics of a one-dimensional thermoacoustic model system governed by the set of equations given in the following. The fields of acoustic pressure $p(x,t)$ and axial particle velocity $u(x,t)$ satisfy

$$\ddot{p} + \alpha \dot{p} - \partial_x (c^2 \partial_x p) = (\gamma - 1)\dot{q}, \tag{6}$$

$$\rho_0 \dot{u} = -\partial_x p, \tag{7}$$

where q is the unsteady component of the volumetric heat release rate, α and γ are (constant) damping coefficient and ratio of specific heats, respectively, ρ_0 is the mean density, and $\dot{(\cdot)}$ denotes a partial derivative with respect to time. The squared acoustic propagation speed is given by $c^2 = \gamma R T$, with the specific gas constant (of air) R taken as constant. Velocity node and pressure node boundary conditions are imposed at the up- and downstream end of the domain (with length L), respectively. We consider a heat source of infinitesimal extent so that the temperature distribution is given by $T = T_1 + \mathrm{H}(x - x_q)(T_2 - T_1)$, where T_1 and T_2 are the temperatures on the unburnt and the burnt side,

respectively, and $\mathrm{H}(x)$ denotes the Heaviside function. To close this system, we need to supply a relation between the acoustic field and the unsteady heat release q. We use

$$q/\bar{q} = n\mathcal{L}_{\mathrm{cd}}[S(u_q)]\,\delta(x - x_q), \tag{8}$$

where n is an interaction index, $\mathcal{L}_{\mathrm{cd}}[\cdot]$ denotes a linear operator representing a convection–diffusion process (defined below), u_q is the normalized acoustic velocity $u/\bar{u}$ at $x \uparrow x_q$, and δ is Dirac's delta function. S is a static saturation nonlinearity, which in the remainder of the paper, will be given by a scaled hyperbolic tangent, $S(u) = \tanh(\sigma u)/\sigma$.

The linear operator $\mathcal{L}_{\mathrm{cd}}$ is defined such that $y(t) = \mathcal{L}_{\mathrm{cd}}[u(t)]$, with $y(t) = \phi(l,t)$, where ϕ is the solution of

$$\dot{\phi} + \bar{u}\partial_x\phi - \Gamma\partial_x^2\phi = 0 \tag{9}$$

with boundary conditions

$$\phi(0,t) = u(t) \quad \text{and} \quad \phi(x,t) < \infty, \quad \text{as } x \to \infty \tag{10}$$

and zero initial conditions. The reason for introducing the operator $\mathcal{L}_{\mathrm{cd}}$ is twofold. First, we model typical flame characteristics by convection (time-lag) and diffusion (low-pass) and, second, we provide, in this way, for non-trivial linear heat release dynamics.

3.2 Linear stability of the model system

To find suitable parameter combinations so that multiple modes are unstable, it is necessary to determine the linear stability characteristics of the model system. This is achieved by well-known frequency domain techniques, shortly summarized below.

Up- and downstream of the heat source, the solution of the acoustic field can be determined. In the present case, we have for admittance and impedance

$$A = -(\rho c)_1^{-1}\frac{1-\exp(-2\mathrm{i}k_1x_q)}{1+\exp(-2\mathrm{i}k_1x_q)}, \quad Z = (\rho c)_2\frac{1+\exp\left(-2\mathrm{i}k_2(L-x_q)\right)}{1-\exp\left(-2\mathrm{i}k_2(L-x_q)\right)}, \tag{11}$$

where subscripts $1,2$ denote evaluation at $T_{1,2}$, the wave numbers on the unburnt and burnt side are given by $k_{1,2} = \left[(\omega/c_{1,2})^2 - \mathrm{i}\alpha\omega/c_{1,2}^2\right]^{1/2}$, and the velocity divergence transfer function for small perturbations reads

$$F_{\mathrm{lin}} = n(T_2/T_1 - 1)\mathcal{F}_{\mathrm{cd}}(\omega). \tag{12}$$

In eqn (12), $\mathcal{F}_{\mathrm{cd}}(\omega)$ is the transfer function of the convection–diffusion operator defined in (9), which, for the boundary conditions (10), can be written as

$$\mathcal{F}_{\mathrm{cd}}(\omega) = \exp\left[Pe/2\left(1-\sqrt{1+4\mathrm{i}\omega\tau Pe^{-1}}\right)\right], \tag{13}$$

where convective time scale and Péclet number are given by $\tau = l/\bar{u}$ and $Pe = \Gamma/(\bar{u}l)$. For assessing linear stability, we do not need to take into account S, since it has unit gain for small amplitudes.

In the following, we fix all parameters (see Tab. 1) except for the convective time τ, which we use to determine the regions of multiple linearly unstable modes. Solutions of the linear dispersion relation (1) were computed for a range of convective time delays. The imaginary parts of the eigenvalues associated with the first three acoustic modes are shown in Fig. 1. There are two intervals of convective time delays in which the first and second mode are both unstable. We will consider the second interval, because in contrast to the first, there are τ values for which the second mode has a larger growth rate than the first and vice versa so that we can observe a broader spectrum of qualitatively different scenarios.

In the next two sections, we will first discuss direct solutions of eqns (6–9) and then apply the harmonic balance approach, presented in Sec. 2, to properly interpret the results.

Table 1: Parameter values for the model system

n	α	T_1	T_2	Pe	$\bar{u}$	σ	L	x_q/L
1/2	$2\pi c_1/100$	300 K	1600 K	0.005	5 m/s	5	1 m	0.6

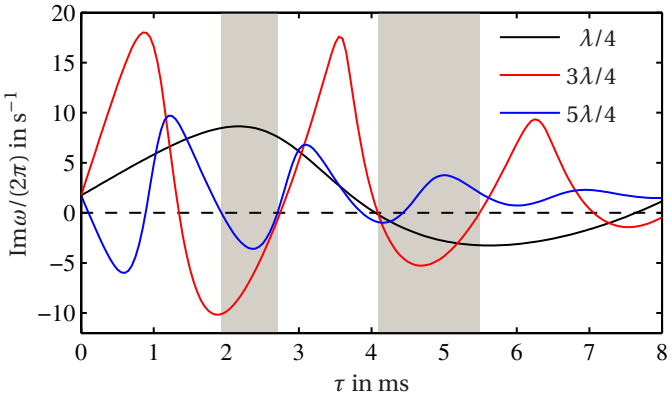

Figure 1: Damping rates of the first three modes as a function of the convective time τ. Shaded regions indicate more than one unstable mode.

3.3 Simulation results

We first set the convective time to 5.2 ms. For this value of τ, the first and second mode have approximately equal linear growth rates (Fig. 1). Two simulations with different initial conditions are considered. In the first, the initial pressure field corresponds to the purely acoustic $\lambda/4$-mode with small amplitude. The acoustic eigenfunctions for a duct with temperature jump can be found, e.g., in Ref. [5]. To identify the two unstable modes in the solution, we project $p(x,t)$ on the purely acoustic eigenfunctions and denote the corresponding amplitudes by $\hat{p}_{\lambda/4}$ and $\hat{p}_{3\lambda/4}$. The acoustic eigenfunctions are not identical to the actual thermoacoustic modes but resemble them sufficiently close so that they can be used to assess the modal contributions in the solution field. The temporal evolution of the amplitudes of the first two acoustic modes and the normalized velocity at the flame are shown in Fig. 2 (left). The first mode grows and settles on a finite amplitude limit cycle whereas the second remains at negligible size. All higher acoustic modes also have a vanishing contribution (not shown).

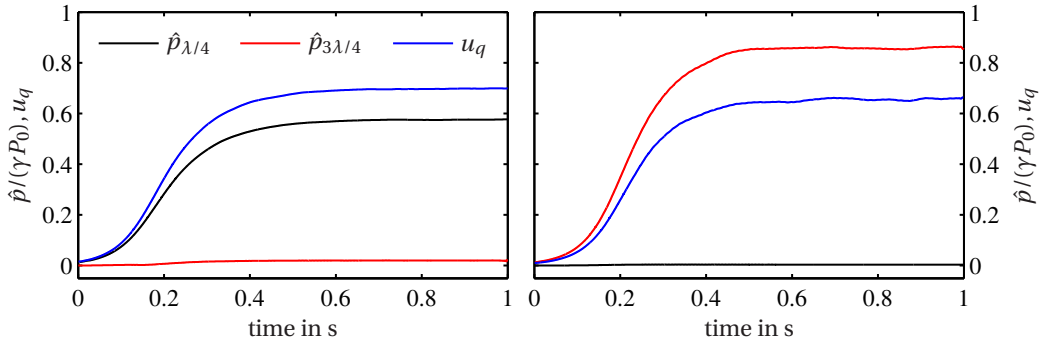

Figure 2: Normalized modal amplitudes and particle velocity at the flame for a convective time τ = 5.2 ms and different initial conditions. Left and right frames correspond to initial perturbations of $\hat{p}_{\lambda/4}$ and $\hat{p}_{3\lambda/4}$, respectively.

The second simulation is run with initial conditions corresponding to the acoustic $3\lambda/4$-mode with small amplitude. This time, the second mode grows and reaches a steady state oscillation (Fig. 2, right);

the first acoustic mode shows negligible contribution. Evidently, for this case, there are two stable equilibrium solutions for fixed system parameters. The initial conditions, in other words, the system's history determines the final oscillation state. A justified question at this point is if there also exists an equilibrium solution which corresponds to simultaneous oscillations of both modes. Using initial conditions composed of different amplitude combinations of the first two modes resulted, however, always in only one of the two modes oscillating in the long time limit (not shown). The describing function analysis in the next section will reveal that there is indeed a two-mode equilibrium solution; it is, however, unstable.

The third simulation was made with a convective time $\tau = 4.8\,\mathrm{ms}$, for which the growth rate of the $3/4\lambda$-mode is larger (see Fig. 1). The initial condition was set to the acoustic $\lambda/4$-mode. We observe significant growth of the corresponding amplitude (Fig. 3) and apparent saturation at a finite level for a distinct period of time. However, at $t = 1\,\mathrm{s}$, the second mode experiences a strong growth, and at the same time, the first mode decreases in amplitude. The second mode continues to grow and, in the end, dominates the long time solution with the first mode being completely suppressed. This behavior is similar to a case shown in Ref. [15]. At this point, however, it is not possible to determine whether a stable $\lambda/4$ oscillation exists and could be realized with different initial conditions.

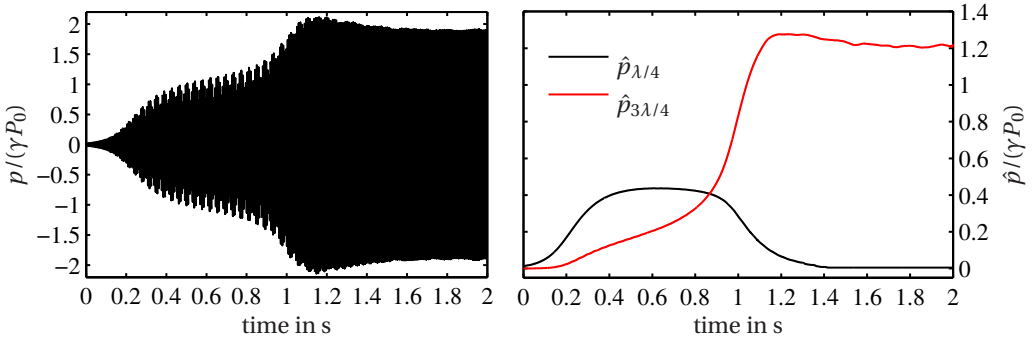

Figure 3: Normalized pressure history at $x = 0$ (left) and modal amplitudes for a convective time $\tau = 4.8\,\mathrm{ms}$

The characteristics observed in the simulation results can be fully explained with the harmonic balance approach for multi-mode oscillations presented in Sec. 2. In addition, this will also provide a clearer picture of the dynamics since all equilibrium solutions and their stability can be assessed.

3.4 Describing function analysis

To explain the results observed in the previous section, we use the harmonic balance approach for multiple unstable modes described in Sec. 2. The definition of the heat release model eqn (8) actually allows us to make a considerable simplification. Since the nonlinearity acts directly on the input of the convection–diffusion operator (see eqn (8)), we can separate the amplitude and frequency dependence of the two. Then we have for two modes $F_{a_1}(\omega_1, \omega_2, a_1, a_2) = F_{\mathrm{lin}}(\omega_1) N_{a_1}(a_1, a_2)$, where F_{lin} is as given in (12), and N is the dual-input describing function associated with the static nonlinearity S. The latter can be computed from its Fourier transform based on an integral identity given in [8], viz.

$$N_{a_1}(a_1, a_2) = \frac{1}{\sigma^2 a_1} \int_{-\infty}^{\infty} \frac{1}{\sinh(\pi s/(2\sigma))} J_0(a_1 s) J_1(a_2 s) \mathrm{d}s, \tag{14}$$

where J_0 and J_1 denote Bessel functions of the first kind of zeroth and first order, respectively. The fundamental harmonic gain for the second input signal follows directly from the symmetrical definition of the dual-input describing function, hence $N_{a_2}(a_1, a_2) = N_{a_1}(a_2, a_1)$.

The dual-input describing function of this saturation type nonlinearity already shows some interesting features (Fig. 4). The gain of the first mode continuously decreases with increasing amplitude of the

second mode. This clearly explains the tendency of one mode suppressing the other. If a_2, for example, is sufficiently large, the gain of a_1 will be so small that the first mode is, in fact, stabilized. (These characteristics are well known in control theory and are extensively used to control nonlinear oscillators by the injection of suitable open-loop signals.)

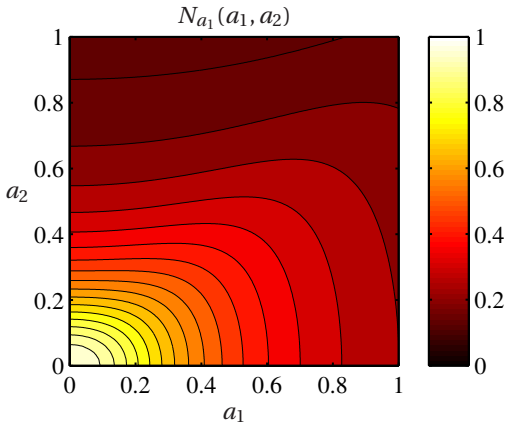

Figure 4: Dual-input describing function of the scaled hyperbolic tangent

For the present case of two unstable modes, the nonlinear dispersion relations read

$$A(\omega_1)Z(\omega_1)[1 + F(\omega_1)N(a_1, a_2)] - 1 = 0, \tag{15a}$$
$$A(\omega_2)Z(\omega_2)[1 + F(\omega_2)N(a_2, a_1)] - 1 = 0, \tag{15b}$$

where we introduced $N = N_{a_1}$ for simplicity. In the following, we will associate a_1 with the $\lambda/4$ and a_2 with the $3\lambda/4$-mode. Calculation of single-mode steady-state oscillations can proceed according to the single-input describing function scenario, with the other amplitude set to zero in (15), and stability is checked by computing the growth rate of the second mode (which does require the dual-input describing function).

For a range of convective times, both single-mode oscillations exist, but they are not always stable (Fig. 5). Depending on τ, only one of the single-mode oscillations is stable or both. A convective time of 5.2 ms lies in the range with two stable equilibrium solutions, consistent with the results of the first simulation in Sec. 3.3. For $\tau = 4.8$ ms, as in the second simulation, the a_1-oscillation is unstable, as expected.

Simultaneous oscillation states need to satisfy eqn (15) and, in addition, $\mathrm{Im}(\omega_1) = \mathrm{Im}(\omega_2) = 0$. When evaluating these conditions, we find that equilibrium solutions with non-zero a_1 and a_2 exist precisely for those values of τ for which both single-mode oscillations are stable. The two-mode oscillations are, however, always unstable. From a topological point of view, the existence of a simultaneous oscillation state in case of stable single-mode equilibria is clear because the two basins of attraction associated with the single-mode oscillations need to be disjoint. Hence, there must be an invariant manifold that separates the two.

It is more instructive to study these dynamical features in an a_1–a_2 phase-plane. Adapting eqn (5) to the present case with two unstable modes, we have

$$\dot{a}_1 = -\mathrm{Im}\big(\omega_1(a_1, a_2)\big)a_1, \tag{16a}$$
$$\dot{a}_2 = -\mathrm{Im}\big(\omega_2(a_1, a_2)\big)a_2, \tag{16b}$$

where the $\omega_{1,2}$ depend on the two oscillation amplitudes through the conditions (15). Based on (16), phase-planes for three different values of τ have been computed (Fig. 6). Consider the left frame, corresponding to a convective time of 5.2 ms, for which both modes have approximately identical growth rates, first. Evidently, the two single-mode steady-state oscillations are stable. In addition, there is an equilibrium state, where the nullclines (representing zero growth in a_1 and a_2) cross, with both modes

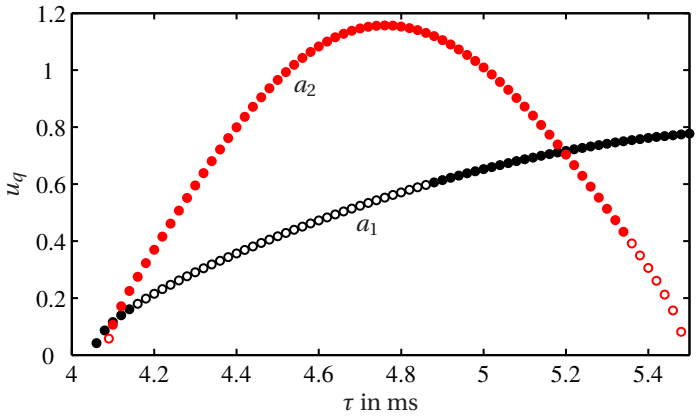

Figure 5: Equilibrium amplitudes of single-mode oscillations as a function of the convective time τ. Filled and open circles correspond to stable and unstable steady-states, respectively.

having finite amplitude. This state represents simultaneous oscillations. However, this equilibrium solution is a saddle point, and therefore, it is unstable. The stable manifold of this saddle point divides the phase-plane into the two basins of attraction of the single-mode oscillations.

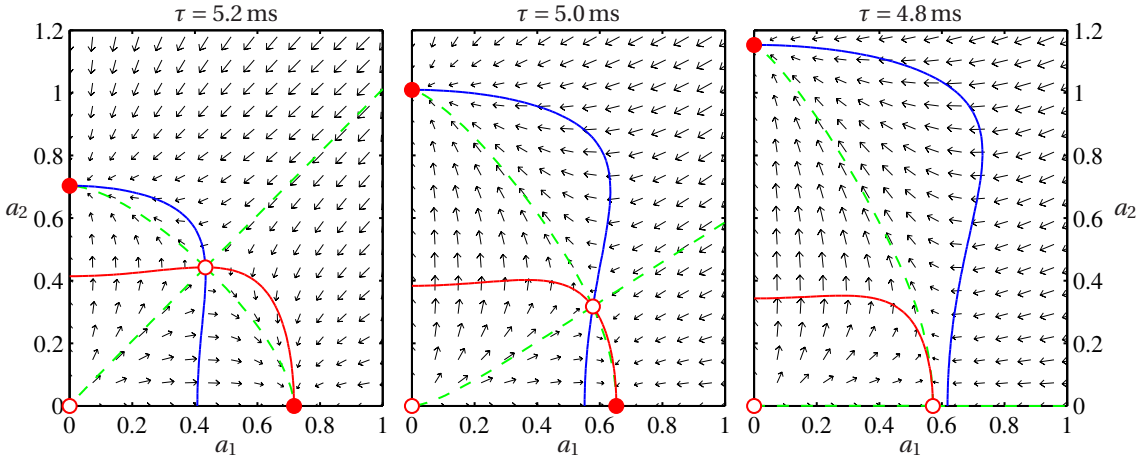

Figure 6: Phase-planes for different values of τ. Stable and unstable equilibrium states are represented by filled and open circles, respectively. Nullclines and the stable and unstable manifolds of the saddle point are shown in addition.

Consider now a decrease in the convective time τ (middle and right frame in Fig. 6). While the amplitudes of the first and second mode decrease and increase, respectively, the saddle point moves closer to the stable fixed point representing the single $\lambda/4$-mode oscillation. At some value of τ, between those for which the phase planes are shown in the middle and right frames, the saddle point collides with the a_1 fixed point. This is, in fact, a subcritical pitchfork bifurcation because the mirror image of the saddle approaches from the lower half-plane also. Then, for the index to remain constant, the three equilibrium states must bifurcate into a saddle.

Increasing the convective time from $\tau = 5.2$ ms has the opposite effect (not shown). The saddle point approaches the a_2 fixed point and eventually collides with it, rendering the single $3\lambda/4$-mode oscillation unstable. If the simultaneous oscillation state exists, the single-mode oscillations are both stable. The long time behavior of the solution then depends on the initial conditions. However, as the saddle point approaches one of the stable fixed points, the respective basin of attraction shrinks, and it will be more difficult to realize this oscillation state.

The right frame in Fig. 6 also explains the simulation result shown in Fig. 3, in which the $\lambda/4$-mode grows significantly and saturates before the second mode eventually dominates. If the initial condition lies close to the stable manifold of the a_1 saddle (Fig. 6, right frame), the system's state is first strongly attracted to this equilibrium solution but then finally repelled to the stable a_2 fixed point.

Consider now again Fig. 5. For a convective time smaller than 4.8 ms, only the a_2 oscillation is stable, and all initial conditions will converge to this state. In a low-noise environment, the system will remain in this state if the convective time is increased up to about $\tau = 5.3$ ms. At this point, the a_2 oscillation becomes unstable, through a collision with the saddle, and the system state will move to the a_1 fixed point, which is now the only attracting set, and will remain on it when further increasing τ. Doing the same now in reverse, the a_2 oscillation persists down to a convective time of about 4.9 ms. Here, the a_2 fixed point becomes unstable, and the system state will move to the a_1 oscillation. This process will be observed as a hysteresis in the oscillation mode, essentially identical to that investigated by van der Pol [22].

4 Discussion & conclusions

In thermoacoustic systems with multiple linearly unstable modes, several stable and unstable equilibrium states may exist. A full assessment of the dynamics in such a system can only be made if the nonlinear heat release response is fairly well known. In the harmonic balance framework presented here, this means that the nonlinearity output for an input signal composed of several sinusoids needs to be available, in other words, a multi-input describing function. As mentioned before, this relation will be excessively laborious to determine for a practical case. On the other hand, the procedure is very clear, and if only two modes have to be considered, the effort may be acceptable.

In principle, a complete dynamical picture can be obtained from a bifurcation analysis based on a time-domain model. There are, however, two major difficulties associated with this approach. First, thermoacoustic dynamics are generally represented by infinite-dimensional systems, and applying a bifurcation analysis tool will require a system of ordinary differential equations. This makes a finite-dimensional truncation of the full equations, typically through a projection on some suitable basis, necessary, and the results will depend on the dimension and the type of the basis. The second point impeding a bifurcation analysis in time-domain, is the complexity of the heat release–acoustic interaction. While the identification of linear heat release models is reasonably well established (see, e.g., various contributions in Ref. [14]), no clear methodology exists, to date, which allows to set-up a nonlinear time-domain model valid for a range of amplitudes and frequencies. Such a model would, however, be required for a time-domain bifurcation analysis.

In studying a thermoacoustic model system, we found two co-existing stable single-mode oscillations. In an a_1–a_2 phase-plane, the basins of attraction of the two were separated by the stable manifold of a saddle point, the latter being associated with simultaneous oscillations. It is the location of this saddle that controls the stability of the single-mode oscillations and the size of their basins of attraction. This emphasizes the need to account for finite amplitude effects caused by both modes simultaneously. For frequency domain methods, this requires a dual-input describing function in the case of two unstable modes. A hysteresis in the oscillation mode, analogous to what we identified in our model system, was also observed in laboratory and test-rig experiments [3, 15]. In Ref. [3], this phenomenon is attributed to thermal effects, but we see that an alternative explanation can be found simply given by the dynamics of two simultaneously unstable modes.

References

[1] D. P. Atherton and H. T. Dorrah. A survey on non-linear oscillations. *Int. J. Control*, 31(6):1041–1105, 1980.

[2] M. Beckmann and G. Himmel. Nonlinear mode competition between unstable drift waves in an rf heated ring discharge. *J. Phys. D: Appl. Phys.*, 31:1695–1705, 1998.

[3] M. Cazalens, S. Roux, C. Sensiau, and T. Poinsot. Combustion instability problems analysis for high pressure jet engine cores. *J. Propul. Power*, 24(4):770–778, 2008.

[4] S. K. Choudhury and A. P. Atherton. Limit cycles in high-order nonlinear systems. *Proc. IEE*, 121(7):717–724, 1974.

[5] A. P. Dowling. The calculation of thermoacoustic oscillations. *J. Sound Vib.*, 180:557–581, 1995.

[6] A. P. Dowling. Nonlinear self-excited oscillations of a ducted flame. *J. Fluid Mech.*, 346:271–290, 1997.

[7] W. J. Dunstan, R. R. Bitmead, and S. M. Savaresi. Fitting nonlinear low-order models for combustion instability control. *Control Eng. Pract.*, 9:1301–1317, 2001.

[8] A. Gelb and W. E. Vander Velde. *Multiple-Input Describing Functions and Nonlinear System Design*. McGraw-Hill, 1968.

[9] E. Gutmark, K. J. Wilson, T. P. Parr, and K. C. Schadow. Feedback control of multi-mode combustion instability. 1992. AIAA paper 92-0778.

[10] X. Huang. *Development of Reduced-Order Flame Models for Prediction of Combustion Instability*. PhD thesis, Virginia Tech, Blacksburg, VI, 2001.

[11] T. Kawahara. Coupled van der Pol oscillators – a model of excitatory and inhibitory neural interactions. *Biol. Cybern.*, 39:37–43, 1980.

[12] T. Lieuwen. Modeling premixed combustion–acoustic wave interactions: A review. *J. Propul. Power*, 19(5):765–781, 2003.

[13] T. C. Lieuwen. Experimental investigation of limit-cycle oscillations in an unstable gas turbine combustor. *J. Propul. Power*, 18(1):61–67, 2002.

[14] T. C. Lieuwen and V. Yang, editors. *Combustion Instabilities in Gas Turbine Engines*, volume 210 of *Progress in Astronautics and Aeronautics*. AIAA, Inc., 2005.

[15] N. Noiray, D. Durox, T. Schuller, and S. Candel. A unified framework for nonlinear combustion instability analysis based on the flame describing function. *J. Fluid Mech.*, 615:139–167, 2008.

[16] A. J. Riley, S. Park, A. P. Dowling, S. Evesque, and A. M. Annaswamy. Advanced closed-loop control of an atmospheric gaseous lean-premixed combustor. *J. Eng. Gas Turbines Power*, 126:708–716, 2004.

[17] J. Schaffner. Simultaneous oscillations in oscillators. *IRE Trans. Circuit Theory*, 1(2):2–8, 1952.

[18] B. Schuermans. *Modeling and Control of Thermoacoustic Instabilities*. PhD thesis, EPF Lausanne, Switzerland, 2003.

[19] B. Schuermans, V. Bellucci, and C. O. Paschereit. Thermoacoustic modeling and control of multi burner combustion systems. 2003. ASME paper 2003-GT-38688.

[20] T. Schuller, N. Tran, N. Noiray, D. Durox, D. Ducruix, and S. Candel. The role of nonlinear acoustic boundary conditions in combustion/acoustic coupled instabilities. 2009. ASME paper GT2009-59390.

[21] S. R. Stow and A. P. Dowling. A time-domain network model for nonlinear thermoacoustic oscillations. *J. Eng. Gas Turbines Power*, 131:031502–1 (9 pages), 2009.

[22] B. van der Pol. On oscillation hysteresis in a triode generator with two degrees of freedom. *Philos. Mag.*, 43(256):700–719, 1922.

[23] B. T. Zinn and T. C. Lieuwen. Combustion instabilities: Basic concepts. In T. C. Lieuwen and V. Yang, editors, *Combustion Instabilities in Gas Turbine Engines*, volume 210 of *Progress in Astronautics and Aeronautics*, pages 3–24. AIAA Inc., 2005.